ACS APPLIED MATERIALS & INTERFACES

Research Article

Cite This: ACS Appl. Mater. Interfaces XXXX, XXX, XXX−XXX

www.acsami.org

Design Molecular Topology for Wet−Dry Adhesion

Jiawei Yang,[†,‡] Ruobing Bai,[†,‡] Jianyu Li,[†,§,∥] Canhui Yang,[†,‡] Xi Yao,[†,‡] Qihan Liu,[†,‡] Joost J. Vlassak,[†] David J. Mooney,[†,§] and Zhigang Suo*[,†,‡]

[†]John A. Paulson School of Engineering and Applied Sciences, [‡]Kavli Institute for Nanobio Science and Technology, and [§]Wyss Institute for Biologically Inspired Engineering, Harvard University, Cambridge, Massachusetts 02138, United States

[∥]Department of Mechanical Engineering, McGill University, Montreal, QC H3A 0C3, Canada

Supporting Information

ABSTRACT: Recent innovations highlight the integration of diverse materials with synthetic and biological hydrogels. Examples include brain−machine interfaces, tissue regeneration, and soft ionic devices. Existing methods of strong adhesion mostly focus on the chemistry of bonds and the mechanics of dissipation but largely overlook the molecular topology of connection. Here, we highlight the significance of molecular topology by designing a specific bond−stitch topology. The bond−stitch topology achieves strong adhesion between preformed hydrogels and various materials, where the hydrogels have no functional groups for chemical coupling, and the adhered materials have functional groups on the surface. The adhesion principle requires a species of polymer chains to form a bond with a material through complementary functional groups and form a network in situ that stitches with the polymer network of a hydrogel. We study the physics and chemistry of this topology and describe its potential applications in medicine and engineering.

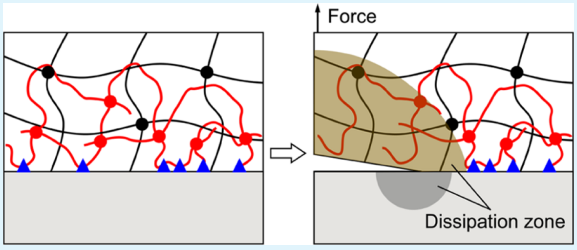

KEYWORDS: *molecular topologies, adhesion, hydrogel, topological entanglement, chemistry of bonds, mechanics of dissipation*

INTRODUCTION

A hydrogel consists of a large amount of water and a polymer network of strong bonds. Integrating synthetic and biological hydrogels with diverse materials is fundamental in many emerging applications, including tissue adhesives,[1−3] medical implants,[4,5] interactive devices,[6,7] water matrix composites,[8−10] chemical sensors,[11,12] and ionotronics.[13−18] Strong adhesion between a hydrogel and another material is often demanded in these applications. However, the abundance of water in the hydrogel poses a particular challenge to its adhesion to the other material: the water molecules in the hydrogel behave like a liquid, changing neighbors constantly and transmitting little load.[16,19] Hydrogels adhere poorly to most materials, either hydrophobic or hydrophilic.[20] Indeed, most hydrogels adhere poorly even to themselves.[21] Rather, strong adhesion relies on the minority constituent of the hydrogel: the polymer network. The sparse polymer network of strong bonds in a hydrogel can (i) transmit significant load through the strong bonds and (ii) elicit dissipation in the bulk of the hydrogel.[22−25] In addition, the abundance of water provides a pathway to the adhesion: the fluidity and the chemistry of water make the hydrogel an ideal host to accommodate various chemical reactions. Hydrogel adhesion is a supramolecular phenomenon and has seen transformative advances in recent years.[19] Strong adhesion is achieved through the synergy of chemistry of bonds, topology of connection, and mechanics of dissipation.[19] Existing methods mostly focus on the chemistry of bonds (e.g., covalent bonds, ionic bonds, and hydrogen bonds)[2,11,21,26,27] and the mechanics of dissipation (e.g., plasticity, viscosity, and distributed damage)[2,13,22,23,27] but largely overlook the topology of connection.

The topology of adhesion refers to a way to connect two materials in space, through bonds, chains, particles, networks, or their combinations. Viewed in this topological perspective, different topologies are needed to achieve strong adhesion, depending on the availability of functional groups for chemical coupling. Take the existing methods as examples: two polymer networks that have complementary functional groups adhere by direct bonding;[23,26,28,29] a polymer network and a nonporous solid that have complementary functional groups adhere by direct bonding;[22] two polymer networks that have noncomplementary functional groups adhere through bonding with nanoparticles[21] or polymer chains[2] that have complementary functional groups; a polymer network and a nonporous solid that have noncomplementary functional groups adhere through bonding with polymer chains that have complementary functional groups;[30,31] two polymer networks that do not have functional groups for chemical coupling adhere by a stitching network.[3,32] Among these methods, forming a direct bond is most widely used, which requires hydrogels to be decorated with functional groups. Decorating hydrogels with functional groups can be realized by

Received: April 29, 2019
Accepted: June 13, 2019
Published: June 13, 2019

DOI: 10.1021/acsami.9b07522
ACS Appl. Mater. Interfaces XXXX, XXX, XXX−XXX

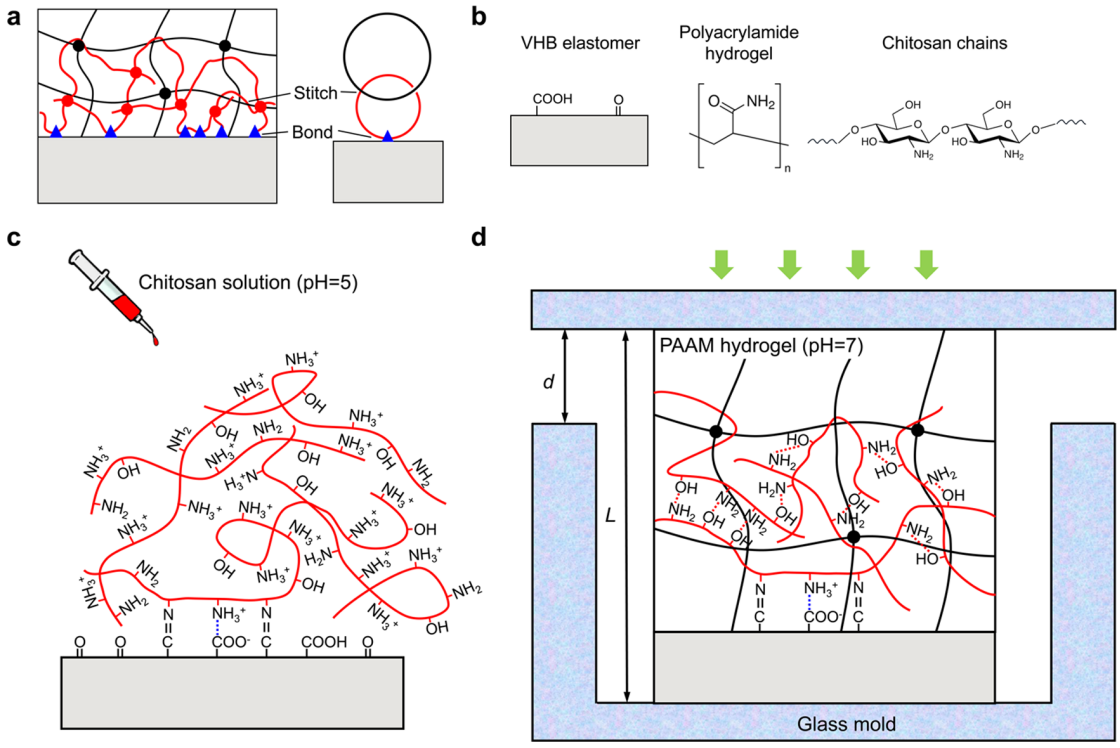

Figure 1. Bond−stitch topology. (a) The surface of a nonporous solid has functional groups amenable to chemical coupling, whereas the polymer network of a hydrogel has no functional groups amenable to chemical coupling. A species of polymer chains bond to the surface of the solid and stitch with the polymer network of the hydrogel. (b) An example of the bond−stitch topology using the following materials: VHB elastomer, polyacrylamide (PAAM) hydrogel, and chitosan chains. (c) When an aqueous solution of chitosan (pH = 5) is spread on the surface of a VHB elastomer, some chitosan chains adsorb on the VHB surface through imine bonds and ionic bonds, and other chitosan chains remain mobile in the solution. (d) When a PAAM hydrogel (pH = 7) is pressed onto the chitosan-coated VHB with a strain $d/L = 7-15\%$, the mobile chitosan chains diffuse into the hydrogel and crosslink into a chitosan network by NH_2−OH hydrogen bonds, localized near the interface and in topological entanglement with the PAAM network.

directly mixing the functional monomers into the hydrogel precursor and subsequently co-polymerizing them to a network with functional moieties. This approach is straightforward and is widely adopted. When the hydrogel is preformed, one can chemically modify the surface of the hydrogel and then link the functional groups onto the network. However, this approach is sophisticated and involves multiple chemical treatments.[33,34] More significantly, many other topologies of adhesion are possible but unexplored (e.g., Figure S1). The diversity of topology would dramatically expand the field with enormous potential for innovation.

To show the potential of topology, here we delve into a simple, hitherto unexplored, topology: a combination of bonds and stitches (Figure 1a). This bond−stitch topology aims to adhere a material (to be called an adherend) and a hydrogel of following characteristics: the surface of the adherend has functional groups amenable to chemical coupling, but the polymer network in the hydrogel has no functional groups for chemical coupling. Both the adherend and the hydrogel are formed before adhesion. These characteristics are often encountered in many applications of adhesion. A species of polymer chains selected to develop the bond−stitch topology should bear functional groups that (i) form bonds with the functional groups on the surface of the adherend and (ii) form a network in situ, in topological entanglement with the polymer network of the hydrogel. The bond and the stitch should have similar breaking strength, which should be comparable to the strength of each adherend to ensure strong adhesion. Strong adhesion is achieved through the synergy of chemistry, mechanics, and topology, and the adhesion energy can approach the fracture energy of the hydrogel. We further study the physics and chemistry of this topology and describe its potential applications in medicine and engineering.

RESULTS AND DISCUSSION

Construction of a Bond−Stitch Topology. We illustrate the bond−stitch topology using three representative components: an acrylic elastomer (VHB 4905, 3 M), a polyacrylamide (PAAM) hydrogel, and chitosan chains (Figure 1b). We choose this adhesion system, because the VHB elastomer finds important applications in soft machines. We first use Fourier-transform infrared spectroscopy (FTIR) to characterize the surface chemistry of the VHB elastomer and identify two functional groups, OH and C═O (Figure S2). Here, we do not rely on FTIR to describe the complete chemistry of VHB elastomer, rather, we aim to look for certain functional groups that can be used to form bonds. Therefore, whether the C═O group belongs to a COOH or a ketone is inconclusive, and we assume that both can exist. Nevertheless, as we will show later, such uncertainty of chemistry does not affect our principle of strong adhesion.

We next investigate the chemistry of the functional groups involved in the adhesion. The pK_a of a carboxylic acid group is ~4.5.[35] The dissociation of charged carboxylic groups, $[COOH] \rightleftarrows [COO^-] + [H^+]$, has an equilibrium constant $K_a = [COO^-][H^+]/[COOH]$. By definition, $pK_a = -\log[K_a]$

DOI: 10.1021/acsami.9b07522
ACS Appl. Mater. Interfaces XXXX, XXX, XXX−XXX

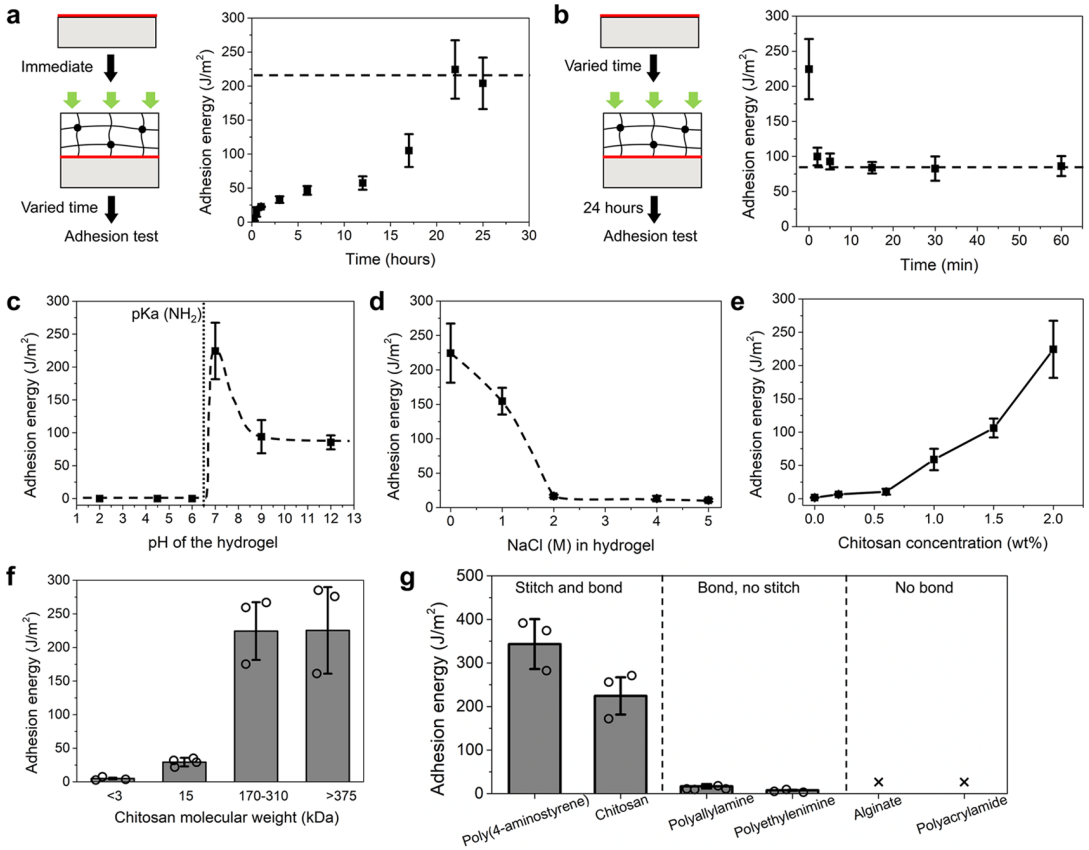

Figure 2. Adhesion energy as a function of several variables. (a) The time after compressing the PAAM hydrogel onto the chitosan-coated VHB. The PAAM hydrogel is compressed on the top immediately after the chitosan solution is spread on the VHB elastomer. (b) The time before compressing the PAAM hydrogel onto the chitosan-coated VHB. The adhesion energy is measured after compressing for 24 h. (c) The pH of the hydrogel. (d) The concentration of salt in the hydrogel. (e) The concentration of chitosan. (f) The molecular weight of chitosan. The concentration of chitosan is fixed at 2 wt %. (g) Polymers that both bond the elastomer and stitch with the hydrogel provide strong adhesion. The lack of either bonds or stitches causes weak adhesion. The polymers used are listed in Table S1. All of the data represent the mean and standard deviation of 3−5 experimental results.

and pH = $-\log[H^+]$. The ratio between the dissociated COO^- and COOH is $[COO^-]/[COOH] = \exp(pH - pK_a)$. When pH < 4.5, $[COO^-] < [COOH]$, the surface is more neutral. When pH > 4.5, $[COO^-] > [COOH]$, the surface is more negatively charged. The PAAM network in the hydrogel has amide groups, which are inert to chemical coupling. The chitosan chains carry amine and hydroxyl groups. The pK_a of an amine group is ∼6.5. The dissociation of charged amine groups, $[NH_3^+] \rightleftarrows [NH_2] + [H^+]$, has an equilibrium constant $K_a = [NH_2][H^+]/[NH_3^+]$. By the same definition, the ratio between NH_2 and the charged NH_3^+ is $[NH_2]/[NH_3^+] = \exp(pH - pK_a)$. When $pH < pK_a = 6.5$, $[NH_2] < [NH_3^+]$, and the chitosan chains dissolve in water as a polyelectrolyte. When pH > 6.5, $[NH_2] > [NH_3^+]$, and the NH_2−OH hydrogen bonds promote the chitosan chains to form a network.[36,37]

The VHB elastomer and the PAAM hydrogel do not have complementary functional groups for chemical coupling and adhere poorly.[20] However, chitosan chains can be used to connect the two materials through the bond−stitch topology. The interfacial bonds between the chitosan and the VHB elastomer can be imine bonds and ionic bonds, formed by the coupling between NH_2 and C═O and between NH_3^+ and COO^-, respectively (amide bond is unlikely to form since the reaction is inactive at room temperature without the catalyst). The optimal pH to form imine bonds is around 4.[38] The availability of NH_3^+ and COO^- at the interface determines the number of formed ionic bonds. The pH to form the chitosan network should be above 6.5. We prepare the chitosan solution of pH = 5 and the PAAM hydrogel of pH = 7.

When an aqueous solution of chitosan of high molecular weight (M_w ∼ 190 000−310 000 Da) and pH = 5 is placed on the surface of the VHB, some chitosan chains adsorb to the VHB surface by forming imine bonds[38,39] and ionic bonds (Figures S3 and S4), and other chitosan chains remain mobile (Figure 1c). When the PAAM hydrogel, pH = 7, is pressed onto the chitosan-coated VHB, the mobile chitosan chains diffuse into the hydrogel and form a network through the NH_2−OH hydrogen bonds, localized near the interface and in topological entanglement with the PAAM network (Figures 1d, S4, and Movies S1 and S2). The mesh size of a hydrogel network is typically on the order of 10 nm, whereas the size of a long-chain chitosan is estimated about 32 nm using the formula $b\sqrt{N}$, where b ∼ 1 nm is the size of the repeat unit of the chitosan chain and N ∼ 1000, the number of repeat unit of a chitosan chain. Even though the size of a chitosan chain is larger than that of the mesh size, the chitosan chains can still manage to interpenetrate into the hydrogel network through the process of reptation.[40] The size of the chitosan chain affects the diffusivity, which can be estimated by the Rouse model $D = kT/(N\eta b)$, where kT is the temperature in the unit of energy, η is the viscosity of water. The smaller molecular weight or shorter chain length leads to larger diffusivity. After

DOI: 10.1021/acsami.9b07522
ACS Appl. Mater. Interfaces XXXX, XXX, XXX−XXX

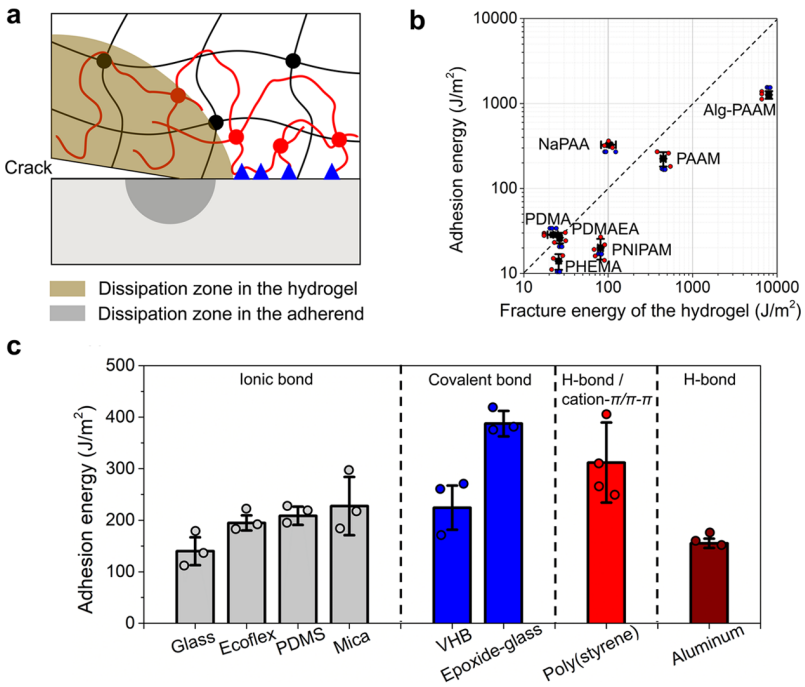

Figure 3. Strong adhesion through the synergy of chemistry, mechanics, and topology. (a) To separate a hydrogel and a material, an external force breaks the bonds as well as causes inelastic dissipation in the bulk. (b) Adhesion energies approach fracture energies of hydrogels. The blue dots represent the data of fracture energies of hydrogels, and the red dots represent the data of adhesion energies. (c) Adhesion energies measured for various adherends. Hydrogels, adherends, and polymer chains are listed in Tables S2 and S3. All of the data represent the mean and standard deviation of 3−5 experimental results.

reaching the thermodynamic equilibrium, the pH at the interface is close to 7, which provides a stable environment to preserve the imine bonds but reduces the ionic bonds due to the neutralization of amines on the chitosan chains. The bond energy of a $NH_3^+-COO^-$ ion pair in water is ∼1−10 kT at room temperature,[41,42] much weaker than that of an imine bond (∼210 kT).[39] Therefore, the strength of interfacial bonds is dominantly contributed by imine bonds. The chitosan network is formed through a collection of NH_2-OH hydrogen bonds among chitosan chains rather than a single hydrogen bond. The equivalent bond energy of such a collection can approach the covalent energy. Therefore, to separate the topological entanglement between the chitosan network and the PAAM network, at least one of the networks must break. The separation of topological entanglement is distinct from the separation of physical entanglement between polymer chains and a polymer network, where the polymer chains can be slowly pulled out by an external force without breaking either material. The adhesion created by this bond−stitch topology is strong, which enables the VHB−chitosan−PAAM system to sustain various types of mechanical loads without separation (Figure S5). We next study the chemistry and physics of this bond−stitch topology and quantify the adhesion energy using the bilayer adhesion test and 90° peel test (Figures S6 and S7).

Characterization of the Bond−Stitch Topology. The bond−stitch topology builds up by three kinetic processes: the formation of imine and ionic bonds between some chitosan chains and the VHB, the diffusion of the mobile chitosan chains into the hydrogel, and the formation of the chitosan network through the NH_2-OH hydrogen bonds. We study the kinetics by measuring the adhesion energy as functions of two durations of time. We first spread the chitosan solution on the VHB surface and immediately press the hydrogel on the top and then measure the adhesion energy as a function of time. The adhesion energy increases initially and reaches a plateau after 20 h (Figure 2a). The data are consistent with the following requirements: the formation of the chitosan network should be slow enough to let the mobile chitosan chains diffuse into the hydrogel and form a network entangled with the hydrogel but not too slow to let all of the mobile chitosan chains diffuse away in the hydrogel, too far apart to form the network. The formation of the imine and ionic bonds between the chitosan chains and the VHB elastomer is much faster than the other two kinetic processes. To test this, we spread the chitosan solution on the VHB, wait for some time before pressing the hydrogel on top, and then measure the adhesion energy after the PAAM−VHB bilayer being pressed for 24 h. The adhesion energy drops quickly when the chitosan solution is present on the VHB surface after 2 min and maintains the same value with even longer wait time (Figure 2b). The reason is probably due to that the longer wait time causes more chitosan chains to anchor on the VHB surface, thus prohibiting the diffusion of chitosan chains into the hydrogel network to form a stitch. Therefore, strong adhesion requires the three kinetic processes to occur concurrently. Any factors that alter even one of the kinetics lead to weak adhesion. For example, if hydrogen bonds are already formed between chitosan chains before compression, the diffusion of the crosslinked chitosan chains into the hydrogel becomes more difficult, which suppresses the stitching process.

The adhesion energy is sensitive to the pH in the hydrogel and peaks at about pH = 7 (Figure 2c). When pH ≪ 7, most NH_2 on chitosan are converted to NH_3^+, and few NH_2-OH hydrogen bonds are present to form the chitosan network. When pH ≫ 7, the chitosan chains rapidly form a network that prohibits the diffusion into the hydrogel; additionally, the high

DOI: 10.1021/acsami.9b07522
ACS Appl. Mater. Interfaces XXXX, XXX, XXX−XXX

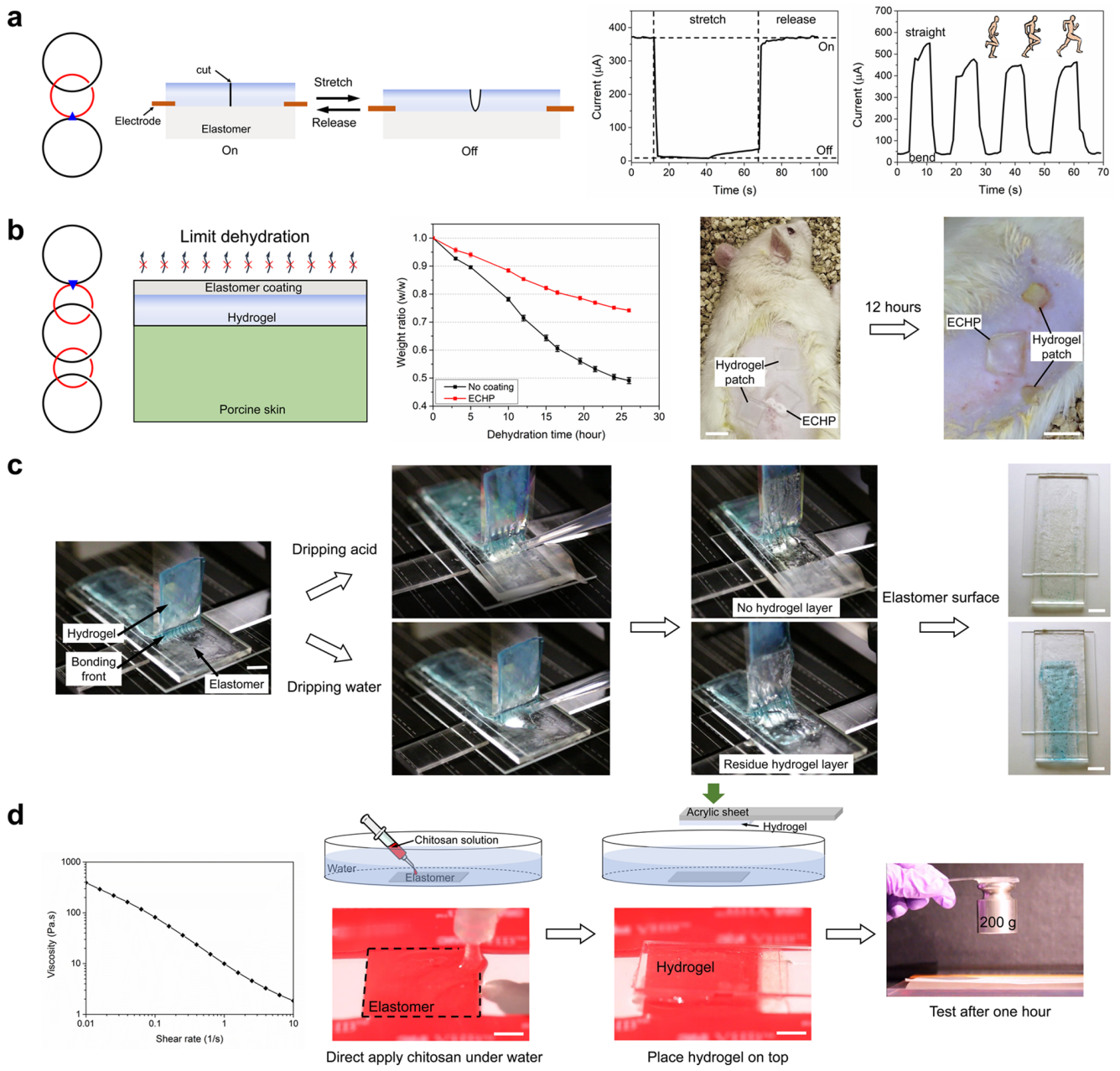

Figure 4. Applications enabled by the bond−stitch topology. (a) Wearable mechanoelectrical transducer. (b) Transparent elastomer-coated hydrogel patch. (c) On-demand loss of adhesion. The blue dye is added to the hydrogel to enhance visualization. (d) Underwater adhesion. The scale bar in (b−d) is 1 cm.

pH value may also interrupt the formation of imine bonds. The adhesion energy is also sensitive to the concentration of salt in the hydrogel, because ionic screening can disturb the formation of both imine and ionic bonds. The adhesion energy exceeds 150 J/m^2 when the concentration of salt is below 1 M but reduces to zero as the concentration of salt is above 2 M, since the high concentrations of sodium and chloride ions provide strong screening and prevent the formation of bond between the functional groups from chitosan and VHB (Figure 2d). Furthermore, the adhesion energy also depends on the concentration and the length of the chitosan chains, since longer and denser chitosan chains are more likely to crosslink into a network that is both resilient and tough (Figure 2e,f).

We confirm that the strong adhesion indeed requires both bonds and stitches. We do so by using several different species of polymer chains (Table S1). Similar to chitosan, poly(4-aminostyrene) (PAS) chains can bond the VHB elastomer and form a network to stitch with the PAAM hydrogel (Figure S8). The adhesion energy is measured above 300 J/m^2 (Figure 2g). In contrast, the adhesion energy of 10 J/m^2 is measured using polyallylamine (PAA) and polyethylenimine (PEI), because both the PAA and PEI chains carry positive charges at the neutral pH (their pK_a values are about 9 and 9.5, respectively),[43,44] and the repulsion between polymer chains fails to form networks to stitch with the hydrogel network. Alginate chains lead to negligible adhesion energy, which is consistent with the previous finding that alginate chains do not

DOI: 10.1021/acsami.9b07522
ACS Appl. Mater. Interfaces XXXX, XXX, XXX−XXX

adhere well with the VHB elastomer,[20] even though the alginate chains form a network that stitches with the PAAM hydrogel.[3] PAAM chains neither bond the VHB elastomer nor stitch with the hydrogel and lead to negligible adhesion energy.

Synergy of Chemistry, Mechanics, and Topology. Adhesion is amplified dramatically by the synergy of chemistry, mechanics, and topology (Figure 3a). As noted before, the VHB elastomer and the PAAM hydrogel by themselves adhere weakly. However, to separate the chitosan-bonded VHB and PAAM, one must break strong bonds. The chitosan and PAAM networks are topologically entangled. The networks of strong bonds transmit the intense stress at the front of the separation into the bulk of the VHB and PAAM and cause inelastic deformation over a large volume of the materials. Here lies the essence of this synergy: the topology elicits strong bonds, which in turn elicits bulk dissipation.

We illustrate this synergy by using hydrogels with various capabilities for dissipation (Table S2). The adhesion energies all approach the fracture energies of the hydrogels (Figures 3b and S9). In particular, an alginate−PAAM hydrogel has two interpenetrating networks: the alginate network of ionic crosslinks and the PAAM network of covalent network. When the hydrogel is stretched, the alginate network unzips and the PAAM network remains intact, leading to pronounced hysteresis and energy dissipation.[24] Here, we find that the dissipation raises the adhesion energy to 1200 J/m^2. A similar amplification of adhesion is demonstrated using chitosan chains to form a bond−stitch topology with a VHB elastomer and an iron-polyacrylate−PAAM hydrogel (Figure S10). We further show that the PAS and chitosan chains adhere the PAAM hydrogel to various materials through several types of bonds (Figures 3c, S11, and Table S3). The glass, Ecoflex (surface modified with COO^-), PDMS (surface modified with COO^-), and mica are all negatively charged on their surfaces, which can form ionic bonds with the positively charged chitosan and PAS chains. To form covalent bonds, in addition to imine bonds, the amine groups on chitosan and PAS can induce ring-opening reaction of epoxide and, thus, form covalent interlinks.[45] The surface of poly(styrene) has phenyl groups, which can form hydrogen bonds, cation−π, and $\pi-\pi$ interactions with the amine and phenyl groups of PAS.[46] The surface of aluminum has an oxide layer, which can form hydrogen bonds with the amine groups of chitosan and PAS.

Applications of the Bond−Stitch Topology. The bond−stitch topology readily integrates various hydrogels and materials to create devices of potential applications in medicine and engineering. We make a wearable mechanoelectrical transducer (Figure 4a). Two pieces of salt-containing PAAM hydrogels adhere to a VHB elastomer using the bond−stitch topology. The salt-containing PAAM hydrogel is an ionic conductor, and the elastomer is a dielectric. When the hydrogels contact each other, an electric current can flow, and the transducer is on. When the hydrogels separate under stretch, the electric current cannot flow, and the transducer is off. We mount the transducer on a knee to monitor the knee flexion during walking, as gait speed directly relates to muscle strength.[47] In one case, the gait speed is measured at ∼10 s/cycle.

We also fabricate a transparent elastomer-coated hydrogel patch (ECHP), in which the elastomer serves to control the rate of dehydration of the hydrogel. Two types of topologies are used to facilitate the adhesion, where the hydrogel adheres to the porcine skin by the stitch−stitch topology and adheres to the elastomer by the bond−stitch topology (Figure 4b). We measure the water loss of the ECHP-skin assembly with time. The ambient temperature is 24 °C, and the relative humidity is 20%. The ECHP-skin assembly loses 25% of total weight and remains soft and transparent after 25 h. Without the elastomer coating, the hydrogel-skin assembly loses more than 50% of the weight and is completely dry (Figure S12). The ECHP is further tested on a rat in vivo (Movie S3). A pure hydrogel patch is included as a control. Both patches are initially firmly bonded to the skin of the rat, despite the movements of the rat. After 12 h, the ECHP is still transparent and remains strongly bonded, whereas the hydrogel patch completely dries out and readily detaches from the skin. The transparency of the ECHP also allows real-time monitor of wound healing.

The bond−stitch topology offers an opportunity to build functions into adhesion. For example, we can break the topology on demand, by changing the pH to below 6.5. At low pH, the chitosan network dissociates, and the imines hydrolyze. We demonstrate the on-demand loss of adhesion using a 90° peeling apparatus. When hydrochloric acid (pH ∼ 1) is dripped on the bonding front, the hydrogel spontaneously detaches from the VHB surface during peeling, and the exposed VHB surface is clean. When the water of pH = 7 is dripped on the bonding front, the hydrogel ruptures during peeling, and a layer of ruptured hydrogel remains on the VHB surface (Figure 4c). This example illustrates a principle: one can design the topology to enable both strong adhesion and easy detachment in response to cues.

The topology further offers possibilities to achieve strong adhesion in environments that are difficult to reach using existing methods. For example, we can adhere to an elastomer and a hydrogel under water (Figure 4d). The chitosan solution is a shear-thinning fluid that can be injected through a syringe and then stay on a surface. We immerse a piece of VHB elastomer in the water, inject the chitosan solution onto its surface through the water, and then immediately press an alg-PAAM hydrogel on the top. After 1 h, the adhered hydrogel-VHB bilayer can sustain a weight of at least 200 g and does not separate even when the weight is intentionally swayed (Movie S4).

CONCLUSIONS

We have described a design principle of adhesion between any hydrogel and any material, to achieve adhesion energy comparable to the fracture energy of the hydrogel. The principle invokes the synergy of chemistry, mechanics, and topology: a topology elicits strong bonds, which in turn elicits bulk dissipation. We demonstrate a bond−stitch topology, study its physics and chemistry, and illustrate its potential uses in medicine and engineering. We show that the adhesion energies can approach the fracture energies of hydrogels themselves and can be as large as 1200 J/m^2. We note that different adhesion testing methods can give different adhesion properties. The testing methods currently used to characterize adhesion usually measure the adhesion properties in terms of the adhesion strength (i.e., the maximum force per unit area) or the adhesion toughness (i.e., the amount of energy needed to advance separation per unit area). For example, probe-pull and lap-shear tests measure the adhesion strength; peel and bilayer-stretch tests measure the adhesion toughness. It is only meaningful to compare values using either adhesion strength or adhesion toughness. Indeed, the two adhesion properties are often in conflict. In particular, the adhesion of high strength

DOI: 10.1021/acsami.9b07522
ACS Appl. Mater. Interfaces XXXX, XXX, XXX−XXX

may not have high toughness. Reconciliation of the conflict between strength and toughness needs further investigation. Bonds and stitches of numerous topologies are unexplored, offering an enormous design space to accommodate different materials and manufacturing processes. The molecular topologies also offer opportunities to build functions into adhesion, such as on-demand loss of adhesion in response to stimuli (e.g., molecules, ions, temperature, and light). The field of innovation is wide open.

EXPERIMENTAL SECTION

Materials. All chemicals were purchased and used without further purification. Monomers for hydrogels included acrylamide (AAm; Sigma-Aldrich, A8887), 2-hydroxyethyl methacrylate (HEMA; Sigma-Aldrich, 128635), *N*-isopropylacrylamide (NIPAM; Sigma-Aldrich, 415324), *N*,*N*-dimethylacrylamide (DMA; Sigma-Aldrich, 274135), acrylic acid (AAc; Sigma-Aldrich, 147230), and [2-(acryloyloxy)-ethyl]trimethylammonium chloride solution (DMAEA; Sigma-Aldrich, 496146). To prepare alg-polyacrylamide tough hydrogels, ionically crosslinkable alginate biopolymer (FMC Biopolymer, Manugel GMB) was used and crosslinked with calcium sulfate slurry (calcium sulfate dihydrate; Sigma-Aldrich, c3771). *N*,*N*′-Methylenebisacrylamide (MBAA; Sigma-Aldrich, M7279) was used as the covalent crosslinker. Ammonium persulfate (APS; Sigma-Aldrich, A9164), sodium persulfate (NaPS, Sigma-Aldrich, 216232), and α-ketoglutaric acid (Sigma-Aldrich, 75890) were used as initiators for polymerization in neutral, alkaline, and acidic environments. *N*,*N*,*N*′,*N*′-tetramethylethylenediamine (TEMED; Sigma-Aldrich, T7024) was used as the crosslinking accelerator for APS and NaPS.

The polymers employed in the study include chitosan chains of four different molecular weights: M_w > 375 000 Da (Sigma-Aldrich, 419419), M_w ∼ 190 000−310 000 Da (Sigma-Aldrich, 448877), M_w ∼ 15 000 Da (Polysciences, 21161-50), and M_w ≤ 3000 Da (Carbosynth, OC28900), poly(4-aminostyrene) (PAS, M_w > 150 000 Da; Polysciences, 02823-1), polyallylamine (PAA, M_w ∼ 58 000 Da; Sigma-Aldrich, 283223), polyethylenimine, branched (PEI, M_w ∼ 25 000 Da; Sigma-Aldrich, 408727), alginic acid sodium salt (M_w ∼ 120 000−190 000 Da, Sigma-Aldrich, 180947), and polyacrylamide (PAAM, M_n ∼ 150 000; Sigma-Aldrich, 767379).

Preparation of Hydrogels. *Polyacrylamide Hydrogels.* Acrylamide powder (40.56 g) was first dissolved in 300 mL of deionized (DI) water, and MBAA was added as a covalent crosslinker (MBAA to acrylamide weight ratio is 0.0006:1). To prepare PAAM hydrogels of pH < 7, α-ketoglutaric acid was used as the UV initiator (α-ketoglutaric acid to acrylamide weight ratio is 0.002:1). The pH of the precursor solution was tuned by dripping HCl solution. The precursor solution was subsequently poured into a glass mold and covered with a 3 mm-thick glass plate and exposed under UV irradiation (30 W, 365 nm curing UV light, McMaster-Carr) for 1 h and set for hours to complete polymerization. To prepare PAAM hydrogels of pH ≥ 7, APS or NaPS was used as the initiator (APS to acrylamide weight ratio is 0.01:1; NaPS to acrylamide weight ratio is 0.007:1), in coupling with TEMED as the crosslinking accelerator (TEMED to acrylamide weight ratio is 0.0028:1). We dripped NaOH to achieve a desired pH. The precursor solution was then poured into a glass mold and covered with a 3 mm-thick glass plate to complete polymerization.

PHEMA Hydrogels. HEMA (46 mL) was dissolved in 200 mL of DI water. We sequentially added MBAA (MBAA to HEMA weight ratio is 0.00033:1), TEMED (TEMED to HEMA weight ratio is 0.002:1), and APS (APS to HEMA weight ratio is 0.0054:1) into the HEMA solution and mixed. The precursor solution was then poured into a glass mold and covered with a 3 mm-thick glass plate to complete polymerization.

PNIPAAM Hydrogels. NIPAM powder (21.52 g) was dissolved in 100 mL of DI water. We sequentially added MBAA (MBAA to NIPAM weight ratio is 0.000377:1), TEMED (TEMED to NIPAM weight ratio is 0.0023:1), and APS (APS to NIPAM weight ratio is 0.006:1) into the NIPAM solution and mixed. The precursor solution was then poured into a glass mold and covered with a 3 mm-thick glass plate to complete polymerization.

PDMA Hydrogels. DMA (4.12 mL) was diluted in 20 mL of DI water. We sequentially added 0.0031 g of MBAA (MBAA to DMA weight ratio is 0.00078:1), TEMED (TEMED to DMA weight ratio is 0.003:1), and APS (APS to DMA weight ratio is 0.0067:1). The precursor solution was mixed and poured into a glass mold and covered with a 3 mm-thick glass plate to complete polymerization.

NaPAA Hydrogels. Acrylic acid (AAc, 8.22 mL) was dissolved in 21.78 mL of DI water. We sequentially added 0.004864 g of MBAA (MBAA to AAc weight ratio is 0.00056:1) and 0.009 g of α-ketoglutaric acid (α-ketoglutaric acid to AAc weight ratio is 0.001:1). We added NaOH to tune the pH of the solution to be neutral. The precursor solution was mixed, poured into a glass mold, and covered with a 3 mm-thick glass plate, exposed under UV irradiation for 1 h and set for hours to complete polymerization.

PDMAEA-Q Hydrogels. DMAEA (16 mL) was dissolved in 14 mL of DI water. We added NaOH to tune the pH of the solution to be neutral. We sequentially added MBAA (MBAA to DMAEA weight ratio is 0.0017:1) and APS (APS to DMAEA weight ratio is 0.0027:1). The precursor solution was then poured into a glass mold and covered with a 3 mm-thick glass plate to complete polymerization.

Alg-PAAM Tough Hydrogels. Acrylamide powder (40.56 g) and 6.78 g of alginate powder were dissolved together in 300 mL of deionized water. We then sequentially added MBAA (MBAA to acrylamide weight ratio is 0.0006:1) and TEMED (TEMED to acrylamide weight ratio is 0.0028:1). The solution was mixed and degassed. Next, we added APS (APS to acrylamide weight ratio is 0.01:1) as the initiator and calcium sulfate slurry as the ionic crosslinker ($CaSO_4$ to acrylamide weight ratio is 0.022:1) into the solution. To prevent fast gelation of alginate, the precursor solution was quickly mixed and immediately poured into a glass mold and covered with a 3 mm-thick glass plate to complete polymerization.

Preparation of Stitching Polymer Solutions. *Chitosan Solution.* 4-Morpholineethanesulfonic acid (MES hydrate; Sigma-Aldrich, M8250) was used to prepare the acidic buffer solution. We first prepared the MES buffer solution by dissolving 0.976 g of MES hydrate powder in 50 mL of DI water and adjusted the pH to 4.5 by titration with NaOH and a pH meter (Mettler Toledo SevenEasy Series Meters). We then added 1 g of chitosan powder (M_w ∼ 190 000−310 000 Da) into the buffer solution and sufficiently stirred with a magnetic stirring bar until the chitosan was completely dissolved. The final pH of the solution was about 5.

PAS Solution. We prepared the MS buffer solution as described above and adjusted the pH to 1 using HCl and a pH meter. We then added 1 wt % PAS into the buffer solution and vigorously mixed. Subsequently, we sonicated the PAS solution in an ultrasonic bath (Branson Ultrasonics) with a constant temperature of 48 °C overnight. After the PAS was completely dissolved, the solution was clear with a deep yellow color. We readjusted the pH of the solution back to 4. All other polymers (PAA, PEI, alginate, and PAAM) were prepared with 2 wt % polymer concentration in either MES buffer solution or water.

Experimental Procedure of Bonding. The prepared polymer solution was directly spread on the surface of an adherend with a thickness of ∼500 μm, calculated by dividing the prescribed volume with the area of the surface. A piece of hydrogel was immediately placed on the top. The bilayer was compressed with strain d/L of 7−15% by customized glass molds. The whole sample was then sealed in a plastic bag to prevent dehydration. The weight of bilayer was measured after 24 h and showed only 0.2 wt % difference, indicating negligible water loss during the procedure.

Study Chitosan Diffusion Using Confocal Microscopy. Fluorescein isothiocyanate (FITC) was purchased from ThermoFisher Scientific, and the fluorescein isothiocyanate-labeled chitosan (FITC-chitosan) was synthesized according to the previously reported protocol.[48] The FITC-chitosan was dissolved in the 4-morpholineethanesulfonic acid (MES) buffer solution (0.1 wt %) with pH adjusted to 5. The solution was covered from light. The polyacrylamide

DOI: 10.1021/acsami.9b07522
ACS Appl. Mater. Interfaces XXXX, XXX, XXX−XXX

hydrogel and the VHB elastomer were subsequently soaked in the FITC-chitosan solution for 1 day. The samples were imaged with a confocal fluorescence microscope (Zeiss LSM710), with the excitation wavelength set to 490 nm and emission wavelength 525 nm. The confocal images were recorded, and three-dimensional constructions were built for analysis. The results showed that the FITC-chitosan chains can diffuse into the hydrogel and form a homogeneous phase but not into the VHB elastomer (Figure S4).

Surface Modification of Silicone Elastomers. The surfaces of silicone elastomers (PDMS, Sylgard 184, and Ecoflex, Smooth-on) were thoroughly cleaned with ethanol and deionized water and dried at room temperature. Following the protocol from ref 23 (Figure S11), the silicone elastomer was soaked in the benzophenone solution (Sigma-Aldrich, B9300) (10 wt % in ethanol) for 10 min to allow benzophenone to adsorb on the surface. The surface was then dried again through an air gun. Next, we placed the elastomer in a mold of the same size, poured an acrylic acid solution (2 M) onto the elastomer, and covered it with a 3 mm-thick glass plate. We subsequently polymerized the acrylic acid under UV irradiation (30 W 365 nm curing UV light, McMaster-Carr) for 1 h. The surface-absorbed benzophenone was excited and would abstract a hydrogen from the surrounding unreactive C−H bonds on the surface of the elastomer, resulting in surface-initiated radicals. The acrylic acid monomers were initiated from the surface and propagated to grow polymer chains, giving rise to a carboxylic acid-modified surface.

Oxygen Plasma Treatment. Glass and aluminum were oxygen plasma-treated before use. Briefly, glass and aluminum sheets were thoroughly cleaned sequentially with acetone, deionized water, ethanol, and isopropyl alcohol and completely dried thereafter. The cleaned samples were subsequently treated by oxygen plasma (SPI Supplies, Plasma Prep II) at an O_2 pressure of 18 psi, vacuum pressure of 275 mTorr, and radio frequency power of 80 W for 120 s. The adhesion was performed immediately after the treatment.

Mechanical Tests. *Bilayer Adhesion Tests.* All tests were conducted in the open air and at room temperature. The preparation and procedure are illustrated in Figure S6. A VHB liner made of polyethylene (PE) was directly used as the stiff backing layer to restrict the deformation of the VHB and the hydrogel beneath it. The bilayer tests were performed on an Instron machine (Instron 3342) with 50 N load cell. The hydrogel was fixed on one grip, and the hydrogel-elastomer bilayer was fixed on the other grip. The loading rate was fixed at 0.2 mm/s. During the tests, the force−stretch curves were recorded, and the critical force and stretch of debonding were identified through a digital camera. The adhesion energy was calculated using formula $G = P(\lambda - 1) - U_s(\lambda)$,[20] where P and λ are the critical force per unit width (the force divided by the width of the sample in the undeformed state) and critical stretch for debonding, $U_s(\lambda)$ is the strain energy stored in the hydrogel divided by the area of the hydrogel in the undeformed state, i.e., the area under the recorded force−stretch curve with stretch from 1 to λ. The typical force−displacement curves are shown in Figure S6d.

90° Peeling Adhesion Tests. All tests were conducted in the open air and at room temperature. The preparation and procedure are illustrated in Figure S7. Peeling tests (90°) were conducted on an Instron machine (Instron 5966) with a 500 N load cell and a 90° peeling apparatus. All adherends were fixed on a moving platform, whereas the hydrogel was glued with a stiff polyester film of thickness 100 μm (clear polyester film, McMaster-Carr) with Krazy glue and fixed to an upper grip. For fixing the VHB elastomer, the VHB elastomer was directly attached on a rigid acrylic plate and mounted on the moving platform. For fixing a mica, the mica was glued on a rigid acrylic plate with Krazy glue and mounted on the moving platform. For fixing a silicone elastomer, we first glued the silicone elastomer on a SBR rubber (Economical Abrasion-Resistant SBR Rubber, McMaster) with a commercially available silicone glue (Sil-Poxy, silicone adhesive, Smooth-on) and then glued the SBR rubber on a rigid acrylic plate with Krazy glue. The entire three layers were mounted on the moving platform. For other adherends, we directly mounted them on the moving platform. The peeling rate was fixed at 0.2 mm/s. We recorded the peeling force as a function of displacement. The adhesion energy was calculated as the average force at plateau divided by the width of the sample.

Pure Shear Tests for Measuring the Facture Energy of Hydrogels. All samples were tested individually on an Instron testing machine (Instron 5966) with a 500 N load cell. The loading rate was fixed at 0.2 mm/s. For each test, two samples of the same hydrogel with dimensions 50 × 10 × 1.5 mm^3 (90 × 10 × 1.5 mm^3 for PAAM hydrogels) were made: one was precut by a crack of 20 mm, and the other was uncut. The uncut sample was used to measure the stress−stretch curve. In the undeformed state, the height of the sample was H; after stretch, the height became λH. We plotted the nominal stress (the force divided by the cross-sectional area of the sample in the undeformed state) as a function of the stretch λ. The area beneath the stress−stretch curve gave the strain energy density stored in the hydrogel, $W(\lambda)$. The precut sample was used to measure the critical stretch λ_c, where the initial crack turned into a running crack. The fracture energy was calculated as $\Gamma = W(\lambda_c)H$.[24,49]

Fabrication of Iron-polyacrylate−PAAM Hydrogel. The procedure is illustrated in Figure S10. Briefly, a PAAM hydrogel was first bonded on a VHB elastomer using the chitosan solution. The sample was immersed in a precursor composed of 2 M AAm, 0.4 M or 0.3 M AAc, and 0.004 M α-ketoglutaric acid in a Petri dish for 1 day, so that the precursor had sufficient time to diffuse into the PAAM hydrogel. The Petri dish with the immersed sample was covered with a polyethylene film and polymerized under UV irradiation for 2 h. The polyethylene film prevented the oxygen inhibition of the polymerization. After polymerization, the precursor became PAAM-*co*-PAAc co-polymers, which interpenetrated with the PAAM network. We then took the sample out and immersed in a 0.06 M $FeCl_3$ reservoir for 2 days. The Fe^{3+} ions diffused into the PAAM hydrogel and crosslinked the PAAM-*co*-PAAc co-polymers by forming coordination complex with the carboxyl groups of the acrylic acid. The hydrogel turned dark brown after the crosslinking process. The sample was subsequently immersed in DI water for 3 days to remove the excess Fe^{3+} ions from the hydrogel.

Fabrication and Test of Wearable Mechanoelectrical Transducer. A PAAM hydrogel containing 1 M sodium chloride was bonded on the surface of an VHB elastomer with the chitosan solution (the concentration was 2 wt %). We subsequently used a razor blade to cut the bonded hydrogel into two strips. The two stripes of hydrogel were attached initially. The resulting structure was connected in a circuit by placing two pieces of aluminum foils in contact with the hydrogels at two ends. We applied an alternating voltage of amplitude 1 V and a frequency of 1 kHz through a signal generator (KEYSIGHT, 33500B) and recorded the electric current via a multimeter (Fluke 8846A). As a voltage was applied, the electric current was measured about 375 μA. When we mechanically stretched the transducer to about double the initial length, the two hydrogels instantly separated but remained firmly bonded on the VHB substrate, and the electric current suddenly dropped to 25 μA. After about 20 s, we released the transducer to its original length, the two hydrogels attached again, and the electric current restored to 375 μA.

Animals. Female Sprague Dawley rats were purchased from Jackson Laboratories and housed at Harvard University. Female Sprague Dawley rats (200−275 g) between 6 and 8 weeks old were used. All studies were carried out in accordance with institutional guidelines approved by Harvard University's Institutional Animal Care and Use Committee (IACUC).

Transdermal Patch Bonded in Vivo on a Rat. The Female Sprague Dawley was anesthetized by inhalation of isoflurane (3−4%), and the dorsum was shaved and disinfected using 70% ethanol. An elastomer-coated hydrogel patch (ECHP) was fabricated by bonding a VHB elastomer with a thickness of 0.5 mm on a piece of PAAM hydrogel using the chitosan solution. The ECHP of dimensions 1 cm × 1 cm × 2 mm was bonded in vivo on the skin of the rat using the chitosan solution and gently pressed for 2 min. A pure hydrogel patch was also included as a control. The rat was then allowed to fully recover from anesthesia on a heating pad. Before returning to the cage, both patches on the skin were inspected and confirmed firmly adhered despite the dynamic movement of the rat. After 12 h, we

DOI: 10.1021/acsami.9b07522
ACS Appl. Mater. Interfaces XXXX, XXX, XXX−XXX

examined both patches in terms of the softness, remaining water, and adhesion.

Measurement of the Viscosity of Chitosan Solution. We measured the viscosity of the chitosan solution of 2 wt % concentration using a rheometer (TA Instruments Discovery HR-3 Hybrid Rheometer) with a cone and plate geometry at a temperature of 25 °C. Flow sweep was used with shear rates ranging from 0.01 to 100 s^{-1}.

Underwater Adhesion. We first attached a VHB elastomer sheet on an acrylic sheet and then glued an alg-PAAM hydrogel on the VHB sheet using the chitosan solution. Another VHB elastomer sheet was attached at the bottom of a Petri dish and immersed in the water. We used a syringe to directly inject a chitosan solution of 2 wt % concentration through the water onto the VHB surface. We immediately covered the alg-PAAM hydrogel on the VHB surface under the water and applied gentle pressure. After 1 h, we took the hydrogel-VHB bilayer out. The VHB liner was peeled off so that the VHB elastomer can adhere with various weights made of stainless steel.

■ ASSOCIATED CONTENT

Supporting Information

The Supporting Information is available free of charge on the ACS Publications website at DOI: 10.1021/acsami.9b07522.

Some other topologies proposed for potential applications; chemistry of the VHB elastomer; formation of imine bonds; chitosan chains can diffuse into the PAAM hydrogel, but not into the VHB elastomer; mechanical robustness of chitosan-bonded PAAM hydrogel and VHB elastomer; bilayer adhesion test; 90° peeling test; chemistry of bonds and stitches with poly(4-aminostyrene); adhesion energy increases with the fracture energy of the PAAM hydrogel; amplification of adhesion energy using an iron-polyacrylate−PAAM hydrogel; surface chemical modification of silicone elastomers; dehydration of hydrogel and elastomer-coated hydrogel patch (ECHP) over time (PDF)

Confocal images of the chitosan distribution in the hydrogel (MOV)

Confocal images of the chitosan distribution in the VHB elastomer (MOV)

Elastomer-coated hydrogel patch and hydrogel patch adhered in vivo on the skin of a rat (MOV)

Underwater adhesion (MOV)

■ AUTHOR INFORMATION

Corresponding Author

*E-mail: suo@seas.harvard.edu.

ORCID

Ruobing Bai: 0000-0002-5847-0502
Canhui Yang: 0000-0001-5674-834X
David J. Mooney: 0000-0001-6299-1194
Zhigang Suo: 0000-0002-4068-4844

Author Contributions

J.Y. and Z.S. conceived the idea to explore molecular topologies of adhesion and wrote the manuscript. J.Y., R.B., J.L., C.Y., and X.Y. carried out experiments and analyzed the experimental data. All authors contributed to the discussion and writing of the manuscript.

Notes

The authors declare no competing financial interest.

■ ACKNOWLEDGMENTS

This work at Harvard was supported by NSF MRSEC (DMR-14-20570). J.L. acknowledges support from Harvard Wyss Institute for Biologically Inspired Engineering and the Natural Sciences and Engineering Research Council of Canada Grant RGPIN-2018-04146.

■ REFERENCES

(1) Bouten, P. J.; Zonjee, M.; Bender, J.; Yauw, S. T.; van Goor, H.; van Hest, J. C.; Hoogenboom, R. The Chemistry of Tissue Adhesive Materials. *Prog. Polym. Sci.* **2014**, *39*, 1375−1405.

(2) Li, J.; Celiz, A.; Yang, J.; Yang, Q.; Wamala, I.; Whyte, W.; Seo, B.; Vasilyev, N.; Vlassak, J.; Suo, Z.; Mooney, D. J. Tough Adhesives for Diverse Wet Surfaces. *Science* **2017**, *357*, 378−381.

(3) Yang, J.; Bai, R.; Suo, Z. Topological Adhesion of Wet Materials. *Adv. Mater.* **2018**, *30*, No. 1800671.

(4) Chin, S. Y.; Poh, Y. C.; Kohler, A.-C.; Compton, J. T.; Hsu, L. L.; Lau, K. M.; Kim, S.; Lee, B. W.; Lee, F. Y.; Sia, S. K. Additive Manufacturing of Hydrogel-Based Materials for Next-Generation Implantable Medical Devices. *Sci. Rob.* **2017**, *2*, No. eaah6451.

(5) Sharma, B.; Fermanian, S.; Gibson, M.; Unterman, S.; Herzka, D. A.; Cascio, B.; Coburn, J.; Hui, A. Y.; Marcus, N.; Gold, G. E.; Elisseeff, J. H. Human Cartilage Repair with a Photoreactive Adhesive-Hydrogel Composite. *Sci. Transl. Med.* **2013**, *5*, No. 167ra6.

(6) Liu, X.; Tang, T.-C.; Tham, E.; Yuk, H.; Lin, S.; Lu, T. K.; Zhao, X. Stretchable Living Materials and Devices with Hydrogel-Elastomer Hybrids Hosting Programmed Cells. *Proc. Natl. Acad. Sci. U.S.A.* **2017**, *114*, 2200−2205.

(7) Liu, X.; Yuk, H.; Lin, S.; Parada, G. A.; Tang, T. C.; Tham, E.; de la Fuente-Nunez, C.; Lu, T. K.; Zhao, X. 3d Printing of Living Responsive Materials and Devices. *Adv. Mater.* **2018**, *30*, No. 1704821.

(8) Huang, Y.; King, D. R.; Sun, T. L.; Nonoyama, T.; Kurokawa, T.; Nakajima, T.; Gong, J. P. Energy-Dissipative Matrices Enable Synergistic Toughening in Fiber Reinforced Soft Composites. *Adv. Funct. Mater.* **2017**, *27*, No. 1605350.

(9) Illeperuma, W. R.; Sun, J.-Y.; Suo, Z.; Vlassak, J. J. Fiber-Reinforced Tough Hydrogels. *Extreme Mech. Lett.* **2014**, *1*, 90−96.

(10) Lin, S.; Cao, C.; Wang, Q.; Gonzalez, M.; Dolbow, J. E.; Zhao, X. Design of Stiff, Tough and Stretchy Hydrogel Composites Via Nanoscale Hybrid Crosslinking and Macroscale Fiber Reinforcement. *Soft Matter* **2014**, *10*, 7519−7527.

(11) Sun, M.; Bai, R.; Yang, X.; Song, J.; Qin, M.; Suo, Z.; He, X. Hydrogel Interferometry for Ultrasensitive and Highly Selective Chemical Detection. *Adv. Mater.* **2018**, No. 1804916.

(12) Qin, M.; Sun, M.; Bai, R.; Mao, Y.; Qian, X.; Sikka, D.; Zhao, Y.; Qi, H. J.; Suo, Z.; He, X. Bioinspired Hydrogel Interferometer for Adaptive Coloration and Chemical Sensing. *Adv. Mater.* **2018**, *30*, No. 1800468.

(13) Wirthl, D.; Pichler, R.; Drack, M.; Kettlguber, G.; Moser, R.; Gerstmayr, R.; Hartmann, F.; Bradt, E.; Kaltseis, R.; Siket, C. M. Instant Tough Bonding of Hydrogels for Soft Machines and Electronics. *Sci. Adv.* **2017**, *3*, No. e1700053.

(14) Lin, S.; Yuk, H.; Zhang, T.; Parada, G. A.; Koo, H.; Yu, C.; Zhao, X. Stretchable Hydrogel Electronics and Devices. *Adv. Mater.* **2016**, *28*, 4497−4505.

(15) Keplinger, C.; Sun, J.-Y.; Foo, C. C.; Rothemund, P.; Whitesides, G. M.; Suo, Z. Stretchable, Transparent, Ionic Conductors. *Science* **2013**, *341*, 984−987.

(16) Yang, C.; Suo, Z. Hydrogel Ionotronics. *Nat. Rev. Mater.* **2018**, *3*, 125−142.

(17) Yuk, H.; Lu, B.; Zhao, X. Hydrogel Bioelectronics. *Chem. Soc. Rev.* **2019**, *48*, 1642−1667.

(18) Lee, H. R.; Kim, C. C.; Sun, J. Y. Stretchable Ionics−a Promising Candidate for Upcoming Wearable Devices. *Adv. Mater.* **2018**, *30*, No. 1704403.

DOI: 10.1021/acsami.9b07522
ACS Appl. Mater. Interfaces XXXX, XXX, XXX−XXX

(19) Yang, J.; Bai, R.; Chen, B.; Suo, Z. Hydrogel Adhesion: A Supramolecular Synergy of Chemistry, Topology, and Mechanics. *Adv. Funct. Mater.* **2019**, No. 1901693.
(20) Tang, J.; Li, J.; Vlassak, J. J.; Suo, Z. Adhesion between Highly Stretchable Materials. *Soft Matter* **2016**, *12*, 1093−1099.
(21) Rose, S.; Prevoteau, A.; Elziere, P.; Hourdet, D.; Marcellan, A.; Leibler, L. Nanoparticle Solutions as Adhesives for Gels and Biological Tissues. *Nature* **2014**, *505*, 382−385.
(22) Yuk, H.; Zhang, T.; Lin, S.; Parada, G. A.; Zhao, X. Tough Bonding of Hydrogels to Diverse Non-Porous Surfaces. *Nat. Mater.* **2016**, *15*, 190−196.
(23) Yuk, H.; Zhang, T.; Parada, G. A.; Liu, X.; Zhao, X. Skin-Inspired Hydrogel-Elastomer Hybrids with Robust Interfaces and Functional Microstructures. *Nat. Commun.* **2016**, *7*, No. 12028.
(24) Sun, J.-Y.; Zhao, X.; Illeperuma, W. R. K.; Chaudhuri, O.; Oh, K. H.; Mooney, D. J.; Vlassak, J. J.; Suo, Z. Highly Stretchable and Tough Hydrogels. *Nature* **2012**, *489*, 133−136.
(25) Gong, J. P.; Katsuyama, Y.; Kurokawa, T.; Osada, Y. Double-Network Hydrogels with Extremely High Mechanical Strength. *Adv. Mater.* **2003**, *15*, 1155−1158.
(26) Liu, Q.; Nian, G.; Yang, C.; Qu, S.; Suo, Z. Bonding Dissimilar Polymer Networks in Various Manufacturing Processes. *Nat. Commun.* **2018**, *9*, No. 846.
(27) Takahashi, R.; Shimano, K.; Okazaki, H.; Kurokawa, T.; Nakajima, T.; Nonoyama, T.; King, D. R.; Gong, J. P. Tough Particle-Based Double Network Hydrogels for Functional Solid Surface Coatings. *Adv. Mater. Interfaces* **2018**, *5*, No. 1801018.
(28) Cha, C.; Antoniadou, E.; Lee, M.; Jeong, J. H.; Ahmed, W. W.; Saif, T. A.; Boppart, S. A.; Kong, H. Tailoring Hydrogel Adhesion to Polydimethylsiloxane Substrates Using Polysaccharide Glue. *Angew. Chem., Int. Ed.* **2013**, *52*, 6949−6952.
(29) Liao, M.; Wan, P.; Wen, J.; Gong, M.; Wu, X.; Wang, Y.; Shi, R.; Zhang, L. Wearable, Healable, and Adhesive Epidermal Sensors Assembled from Mussel-Inspired Conductive Hybrid Hydrogel Framework. *Adv. Funct. Mater.* **2017**, *27*, No. 1703852.
(30) Sudre, G.; Olanier, L.; Tran, Y.; Hourdet, D.; Creton, C. Reversible Adhesion between a Hydrogel and a Polymer Brush. *Soft Matter* **2012**, *8*, 8184−8193.
(31) Macron, J.; Bresson, B.; Tran, Y.; Hourdet, D.; Creton, C. Equilibrium and out-of-Equilibrium Adherence of Hydrogels against Polymer Brushes. *Macromolecules* **2018**, *51*, 7556−7566.
(32) Gao, Y.; Wu, K.; Suo, Z. Photodetachable Adhesion. *Adv. Mater.* **2018**, *31*, No. 1806948.
(33) Yao, X.; Chen, L.; Ju, J.; Li, C.; Tian, Y.; Jiang, L.; Liu, M. Superhydrophobic Diffusion Barriers for Hydrogels Via Confined Interfacial Modification. *Adv. Mater.* **2016**, *28*, 7383−7389.
(34) Ohsedo, Y.; Takashina, R.; Gong, J. P.; Osada, Y. Surface Friction of Hydrogels with Well-Defined Polyelectrolyte Brushes. *Langmuir* **2004**, *20*, 6549−6555.
(35) Chollakup, R.; Smitthipong, W.; Eisenbach, C. D.; Tirrell, M. Phase Behavior and Coacervation of Aqueous Poly (Acrylic Acid)-Poly (Allylamine) Solutions. *Macromolecules* **2010**, *43*, 2518−2528.
(36) Okuyama, K.; Noguchi, K.; Miyazawa, T.; Yui, T.; Ogawa, K. Molecular and Crystal Structure of Hydrated Chitosan. *Macromolecules* **1997**, *30*, 5849−5855.
(37) Ladet, S.; David, L.; Domard, A. Multi-Membrane Hydrogels. *Nature* **2008**, *452*, 76−79.
(38) Fessenden, R. J.; Fessenden, J. S. *Organic Chemistry*, 2nd ed.; Willard Grant Press: Boston, 1982.
(39) Layer, R. W. The Chemistry of Imines. *Chem. Rev.* **1963**, *63*, 489−510.
(40) Doi, M.; Edwards, S. F. *The Theory of Polymer Dynamics*; Oxford University Press: New York, 1988.
(41) Nagy, P. I.; Erhardt, P. W. On the Interaction of Aliphatic Amines and Ammonium Ions with Carboxylic Acids in Solution and in Receptor Pockets. *J. Phys. Chem. B* **2012**, *116*, 5425−5436.
(42) Berg, J. M.; Tymoczko, J. L.; Stryer, L.; Berg, J.; Tymoczko, J.; Stryer, L. *Biochemistry*; W. H. Freeman: New York, 2002.
(43) Kozlovskaya, V.; Kharlampieva, E.; Jones, K.; Lin, Z.; Tsukruk, V. V. pH-Controlled Assembly and Properties of Lbl Membranes from Branched Conjugated Poly (Alkoxythiophene Sulfonate) and Various Polycations. *Langmuir* **2009**, *26*, 7138−7147.
(44) Cranford, S. W.; Ortiz, C.; Buehler, M. J. Mechanomutable Properties of a Paa/Pah Polyelectrolyte Complex: Rate Dependence and Ionization Effects on Tunable Adhesion Strength. *Soft Matter* **2010**, *6*, 4175−4188.
(45) Stropoli, S. J.; Elrod, M. J. Assessing the Potential for the Reactions of Epoxides with Amines on Secondary Organic Aerosol Particles. *J. Phys. Chem. A* **2015**, *119*, 10181−10189.
(46) Meyer, E. A.; Castellano, R. K.; Diederich, F. Interactions with Aromatic Rings in Chemical and Biological Recognition. *Angew. Chem., Int. Ed.* **2003**, *42*, 1210−1250.
(47) Thoumie, P.; Mevellec, E. Relation between Walking Speed and Muscle Strength Is Affected by Somatosensory Loss in Multiple Sclerosis. *J. Neurol., Neurosurg. Psychiatry* **2002**, *73*, 313−315.
(48) Qaqish, R. B.; Amiji, M. M. Synthesis of a Fluorescent Chitosan Derivative and Its Application for the Study of Chitosan-Mucin Interactions. *Carbohydr. Polym.* **1999**, *38*, 99−107.
(49) Rivlin, R.; Thomas, A. Rupture of Rubber. I. Characteristic Energy for Tearing. *J. Polym. Sci.* **1953**, *10*, 291−318.

DOI: 10.1021/acsami.9b07522
ACS Appl. Mater. Interfaces XXXX, XXX, XXX−XXX